


LETTER

Ephemeral aggregate layers in the water column leave lasting footprints in the carbon cycle

Jennifer C. Prairie ¹* Kai Ziervogel,^{2,a}* Roberto Camassa,³ Richard M. McLaughlin,³ Brian L. White,² Zackary I. Johnson,⁴ Carol Arnost²

¹Department of Environmental and Ocean Sciences, University of San Diego, San Diego, California; ²Department of Marine Sciences, University of North Carolina at Chapel Hill, Chapel Hill, North Carolina; ³Carolina Center for Interdisciplinary Applied Mathematics, Department of Mathematics, University of North Carolina at Chapel Hill, Chapel Hill, North Carolina; ⁴Nicholas School of the Environment and Biology Department, Duke University Marine Lab, Beaufort, North Carolina

Scientific Significance Statement

The large-scale transfer of phytoplankton-derived organic carbon from the surface ocean to depth (the “biological pump”) occurs via sinking aggregates that are colonized by heterotrophic bacteria, making them hotspots for organic matter remineralization. Using laboratory experiments with diatom aggregates in a stratified water column, we demonstrated that aggregate thin layers, such as those commonly found in the coastal ocean, are regions of increased microbial concentration and rates of heterotrophic activity. This enhanced bacterial concentration and activity persisted long after the marine snow aggregates passed through the density interface, suggesting that these small-scale interactions within aggregate thin layers can affect carbon cycling in the water column on much larger temporal and spatial scales.

Abstract

Marine aggregates play a critical role in the biological pump, both as a dominant component of carbon flux and as hotspots for organic matter remineralization by microbial communities. In this study, we used laboratory experiments to investigate how aggregate thin layers, such as those commonly found in the coastal ocean, affect the distribution of bacteria and their activity. Diatom aggregates were added to a stratified water column, forming layers within which both microbial concentration and extracellular enzyme activity were substantially increased relative to background levels. Importantly, this enhancement of bacterial concentration and activity persisted long after the marine snow aggregates settled through the tank—that is, 10 times longer than the duration of the aggregate layer at the density interface. Thus, these small-scale microbial interactions within aggregate layers leave behind considerable “carbon processing footprints” in the water column that may affect biogeochemical cycles at much larger temporal and spatial scales.

*Correspondence: jcp Prairie@san Diego.edu and kai.ziervogel@unh.edu

Author Contribution Statement: JCP, KZ, CA: designed experiments. JCP, KZ: carried out experiments and analyzed data. ZJ: analyzed additional data. JCP, KZ, CA, RC, RLM, BLW, ZJ: discussed results. JCP, KZ, CA, with input from all other co-authors: wrote manuscript.

Data Availability Statement: Data from this study are available on figshare at <https://doi.org/10.6084/m9.figshare.5143261>.

^aPresent address: Institute for the Study of Earth, Oceans, and Space, University of New Hampshire, New Hampshire

Additional Supporting Information may be found in the online version of this article.

This is an open access article under the terms of the Creative Commons Attribution License, which permits use, distribution and reproduction in any medium, provided the original work is properly cited.

The sinking flux of organic matter from the surface ocean to depths below the pycnocline drives the biological pump, which contributes to the transfer of CO₂ from the atmosphere to the ocean (Passow and Carlson 2012). This removal process is facilitated by sinking aggregates, which dominate the flux of photosynthetically fixed carbon to the deep ocean (Ducklow et al. 2001; Turner 2015). These aggregates are hotspots of specialized heterotrophic microbial communities that facilitate the transformation and remineralization of organic matter in the water column (DeLong et al. 1993; Arnosti 2011). Aggregate-associated bacteria often are present at concentrations that are orders of magnitude higher than in the surrounding seawater, with higher metabolic rates (Ploug and Grossart 2000; Grossart et al. 2007) and hydrolytic enzyme activities (Smith et al. 1992; Ziervogel and Arnosti 2008) than neighboring non-aggregate-attached bacteria. This tight coupling between aggregates and heterotrophic bacteria leads to small-scale heterogeneity in the distribution of bacteria, and thus the remineralization of organic matter in the ocean (Azam and Long 2001).

Sinking aggregates are also heterogeneously distributed in the ocean: aggregates can form thin layers, which can extend for kilometers and persist for days (Alldredge et al. 2002; McManus et al. 2003). Studies have found that aggregate thin layers can be common in coastal waters and may form by a variety of mechanisms, including shear-thinning of existing horizontal patches (Franks 1995) and delayed settling, that is, decreases in settling velocity as aggregates sink through sharp density gradients (MacIntyre et al. 1995; Camassa et al. 2013; Prairie et al. 2013). Unlike other mechanisms, velocity changes associated with sharp stratification act to temporarily trap settling particles (Prairie et al. 2013) or buoyant jets such as rising oil plumes (Camassa et al. 2016), increasing local concentration above initial values. Thus, delayed settling may play a particularly important role in affecting vertical aggregate distributions, and can result in the formation of thin layers that are both peaky and asymmetrical in shape (Prairie and White 2017).

Therefore, depending on the mechanism of formation, these aggregate layers can be regions of considerably enhanced particle concentrations—with peak concentrations often an order of magnitude higher than background levels above or below the layer—over relatively thin vertical spans of less than a few meters (Alldredge et al. 2002). Such thin layers have the potential to affect carbon cycling, as well as biogeochemical cycling of other elements, at much larger spatial and temporal scales than individual sinking aggregates. Recent studies measuring enhanced microbial activity associated with marine snow particles have suggested that these effects should be magnified in highly concentrated aggregate layers (Prairie et al. 2015). However, although enhanced bacterial concentrations and activities have been explored theoretically and experimentally within the plumes of individual sinking aggregates (Kjørboe and Jackson 2001;

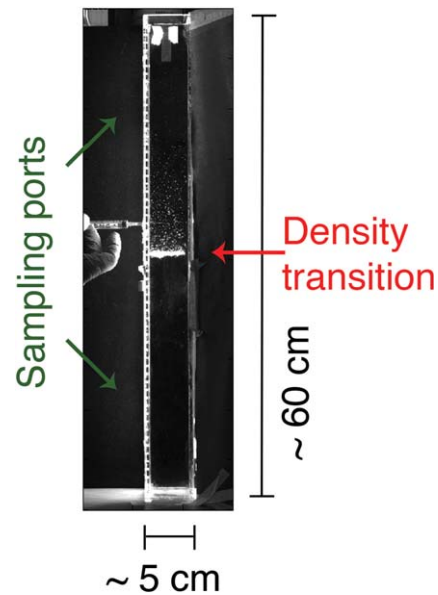


Fig. 1. Image from Exp. 2 (Stratified artificial seawater) showing experimental setup.

Stocker et al. 2008), the specific effects of aggregate layers on bacterial communities and their carbon cycling activities have not been directly examined experimentally.

Here, we use a novel experimental setup to determine the effect of an ephemeral aggregate thin layer on microbially driven carbon cycling. Thin layers were formed in the lab by delayed settling of particles at a sharp density gradient. We investigated the effects of these layers on the spatial and temporal distribution of microbial cells and on the activities of extracellular enzymes used in the initial step of microbially driven carbon cycling (Arnosti 2011). Within the aggregate layer, we observed substantially enhanced bacterial concentrations and enzymatic hydrolysis rates, which lasted for more than 1.5 h, long after all particles had settled through the density gradient. The prolonged persistence of the elevated cellular concentration and enzymatic hydrolysis rates demonstrates that relatively ephemeral aggregate layers (which lasted for less than 10 min in our experiments but can last for over a day in the coastal ocean) can affect carbon cycling dynamics on much longer temporal scales than that of the layers themselves.

Methods

Aggregate thin layers were produced in the lab by adding diatom aggregates to a rectangular tank (~ 60 cm tall and with a 5 × 5 cm base) that was stratified with a sharp vertical salinity gradient (Fig. 1). One side of the tank had silicon-stoppered sampling ports at approximately 1 cm intervals (visible in Fig. 1); these ports allowed for subsamples to be collected from discrete depths for analysis of cell concentrations and extracellular enzyme activities without

disturbing the stratification or distribution of aggregates within the tank (see below). The top layer of the tank contained an artificial seawater (ASW) solution, prepared with Instant Ocean (Spectrum Brands), with a salinity of ~ 20 PSU; the bottom layer contained an ASW solution of ~ 36 PSU. Both solutions were filtered through a $0.1\text{-}\mu\text{m}$ polycarbonate filter using low vacuum prior to filling the tank. This procedure was sufficient to remove most bacterial cells, but the ASW solution was not sterile, and low but detectable numbers of bacterial cells were present in solution prior to introduction of aggregates (see Supporting Information Table 2).

A sharp density gradient was created in the tank by slowly pouring the top layer fluid through a diffuser (Prairie et al. 2013). Two experiments with aggregates were conducted using a stratified tank (Exp. 1 and Exp. 2) in addition to a control experiment in which aggregates were added to an unstratified tank filled with an ASW solution of 20 PSU (Exp. 3). Another control experiment was conducted in which no aggregates were added to a stratified tank (Exp. 4; see Supporting Information Table 1).

Aggregates were produced in roller tanks (Shanks and Edmondson 1989; Jackson 2004) filled with mixed diatom cultures that were added to either unfiltered near-shore seawater (SW) or artificial seawater (ASW) (see Supporting Information Table 1). Coastal seawater (SW) was collected on Pawley Island, South Carolina, U.S.A. (33.47° N, 79.10° W; Salinity: 34 PSU; Water temperature: 26°C), and kept aerated at room temperature for 5 d in the laboratory prior to the roller tank incubations. The mixed senescent diatom culture was prepared by combining aliquots of seven diatom monocultures (*Fragilariopsis* sp., *Thalassiosira* sp., *Pseudo-nitzschia* sp., *Chaetoceros* sp., *Cylindrotheca* sp., *Skeletonema* sp., *Phaeodactylum* sp.) in a glass bottle before being combined with SW or ASW to completely fill the roller tanks (total volume ~ 4.5 L, see Supporting Information Table 1 for ratios for each experiment). Monocultures of the seven diatoms were maintained under non-axenic conditions at 12°C and constant light (Aquil media). Note that, since the composition of diatom-associated bacterial communities varies by diatom species as well as by diatom growth phase (Grossart et al. 2005), the bacterial composition of the inoculum likely varied between experiments.

Once filled, roller tanks were rotated at 3.5 rpm at room temperature for 2–3 d, depending on the experiment (see Supporting Information Table 1). Millimeter-sized aggregates formed within hours after the start of all incubations, and aggregate formation continued until the end of the incubations. Roller tanks were then placed upright on the bench to let aggregates settle to the bottom of the tank. Aggregates were carefully removed from the tanks using a 1-mL cut-off syringe and placed into clean 20-mL scintillation glass vials containing ASW at ~ 20 PSU. Diatom aggregates formed in SW were allowed to equilibrate to the lower salinity fluid

(~ 20 PSU) for 1 h prior to initiation of the experiments in the sinking tank. This equilibration period is intended to allow higher density seawater within the aggregates to exchange with the lower density surrounding fluid (Prairie et al. 2015).

A total volume of 5 mL of the aggregates was then transferred to the rectangular tank and carefully released below the tank air–water interface. For each aggregate sinking experiment, continuous images were recorded using a Pike F-100B camera (Allied Vision Technologies, Germany) at a rate that was constant for an experiment, but ranged between 12 and 25 frames s^{-1} between experiments. The images captured the entire tank in the field of view, and images were taken for at least 8 min after the aggregates were added. The images were processed using MATLAB, first subtracting from each image a baseline image taken before aggregates were added. The intensity of a corrected image was then summed at each depth to determine particle intensity vs. depth for each image. These profiles were normalized by the maximum particle intensity observed throughout the experiment (summed over all depths of the tank) to obtain relative particle intensity as a fraction of the maximum vs. both time and depth. These profiles of relative particle intensity provide a proxy for particle concentration vs. depth and time.

Subsamples (~ 2 mL of water) were collected at seven distinct depths (Supporting Information Table 2) from the sampling ports in the side of the tank before aggregates were added, while the aggregates were sinking (Fig. 1), and after the aggregates had settled to the bottom of the tank (see Supporting Information Table 2 for specific sampling depths and time points, as well as cell counts and enzyme activities). Samples were collected using a 3-mL plastic syringe equipped with a needle introduced horizontally into the tank through the silicon-sealed sampling ports (see Fig. 1, which shows a sample being collected). Shortly after collection, the samples were gently centrifuged at 194 g (the lowest setting on an Eppendorf MiniSpin, sufficiently low to avoid cell lysis) for 1 min to remove large fractions of aggregates that were visible in some of the samples. The supernatant was used for measurements of extracellular enzymatic activity, cell concentrations, and salinity, as described below. Despite the fact that the samples were gently centrifuged, it is possible that small fractions of aggregates remained in some samples, which could have affected these measurements.

Extracellular enzyme activity was measured using L-leucine-4-methylcoumarinyl-7-amide (MCA) hydrochloride as substrate proxy for leucine-aminopeptidase activity (final concentration: $350\ \mu\text{M}$) according to Hoppe (1983). Incubations were conducted in disposable acrylic cuvettes ($700\ \mu\text{L}$ incubation solution) at room temperature in the dark. Changes in fluorescence over time were monitored four times over an incubation time of 1 h using a Turner Biosystems TBS-380 fluorometer, with excitation/emission channels set to “UV” (365 nm excitation, 440–470 nm emission).

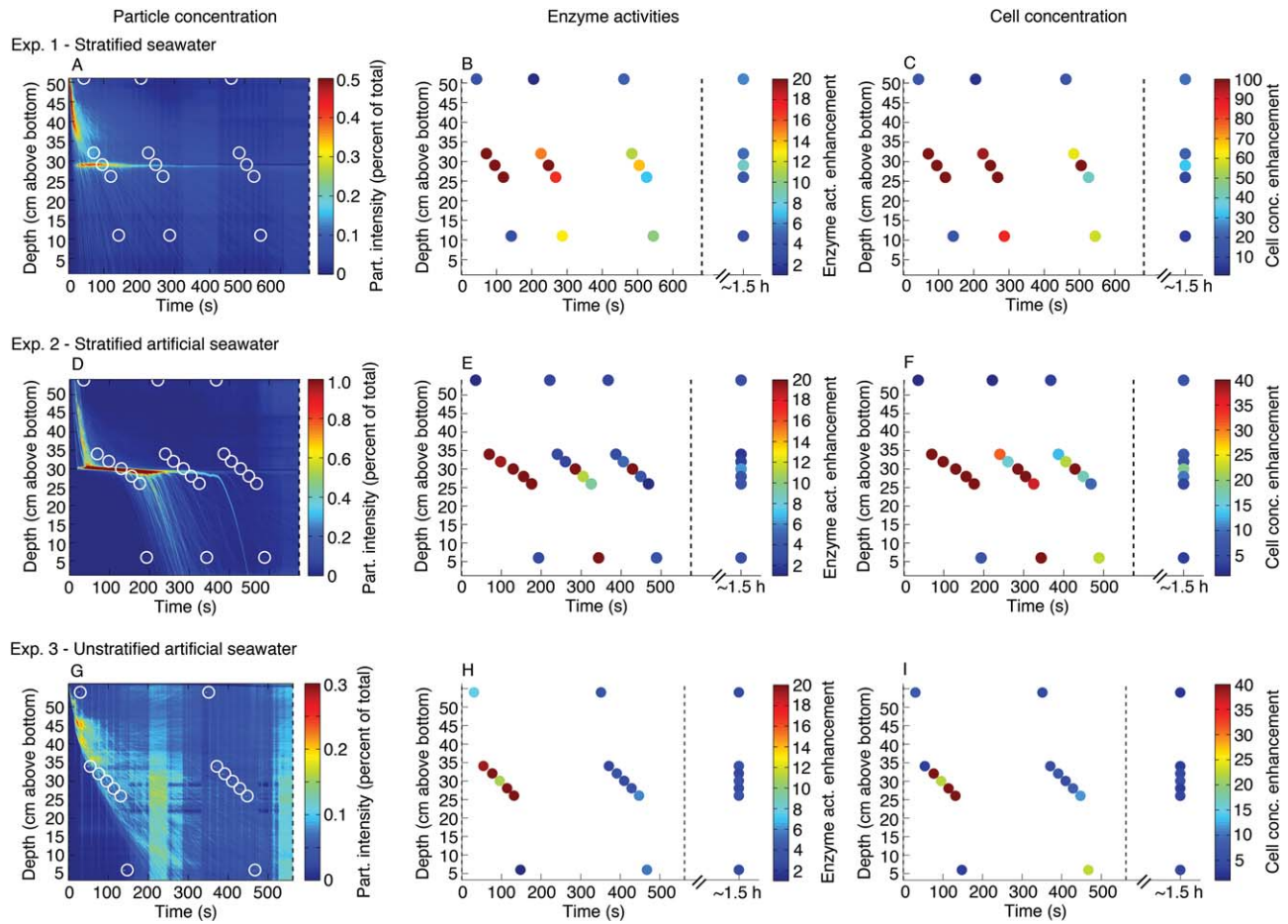


Fig. 2. Two aggregate settling experiments were performed in stratified tanks: Exp. 1 with aggregates formed from diatoms mixed with coastal seawater (A–C) and Exp. 2 with aggregates formed from diatoms mixed with artificial seawater (D–F). One experiment was performed in an unstratified tank with aggregates formed from diatoms mixed with artificial seawater (G–I). (A, D, G) shows particle intensity vs. time and depth. In stratified experiments, particle intensity is enhanced at the density interface, indicating the presence of an aggregate layer for 100s of seconds. Corresponding enhancements of microbial enzyme activity (B, E) and microbial cell concentrations (C, F) are also shown vs. time and depth. Both microbial enzyme activity and cell concentrations are enhanced at the depth of the layer even ~ 1.5 h after the aggregates were added. In the unstratified experiment, particle intensity initially is spread over a broader depth interval (G), and little enhancement in enzyme activity (H) or cell concentrations (I) is observed in the water column at either ~ 400 s or ~ 1.5 h after aggregate addition. White circles in (A, D, G) show times and depths at which samples were taken which correspond to colored circles in (B, C, E, F, H, I). Enhancements were calculated by dividing by the median baseline value (taken before aggregates were added).

Fluorescence changes were calibrated using an MCA standard solution.

Bacterioplankton were counted using flow cytometry following the procedures described in Johnson et al. (2010) and Lin et al. (2013). One milliliter of water was fixed with 25% buffered formalin (0.125% final concentration) and stored in 2-mL Eppendorf tubes at -80°C until analysis (no longer than 3 months). Shortly before analysis, fixed samples were thawed in a cooler on blue ice. Bacterial cells were stained with SYBR-Green I ($1\times$ final concentration; Marie et al. 1999), kept on ice in the dark for 30 min, and enumerated on a FACSCalibur flow cytometer (Becton Dickinson) modified with a syringe pump for quantitative sample delivery.

In the stratified experiments, salinity measurements confirmed the presence of a sharp salinity gradient, which persisted throughout the duration of the experiment (Supporting Information Fig. 1). Salinity was measured using a hand held refractometer ($10\ \mu\text{L}$ sample volume) at each sample time and depth, with the exception of Exp. 1 (the stratified experiment which used aggregates formed in near-shore seawater). For Exp. 1, tank water salinity was measured ~ 30 min after the final sample was taken with a MicroScale Conductivity and Temperature Instrument (Precision Measurement Engineering).

For each time and depth, enhancements in bacterial cell counts and rates of enzyme activities were calculated by normalizing by baseline values measured before aggregates were

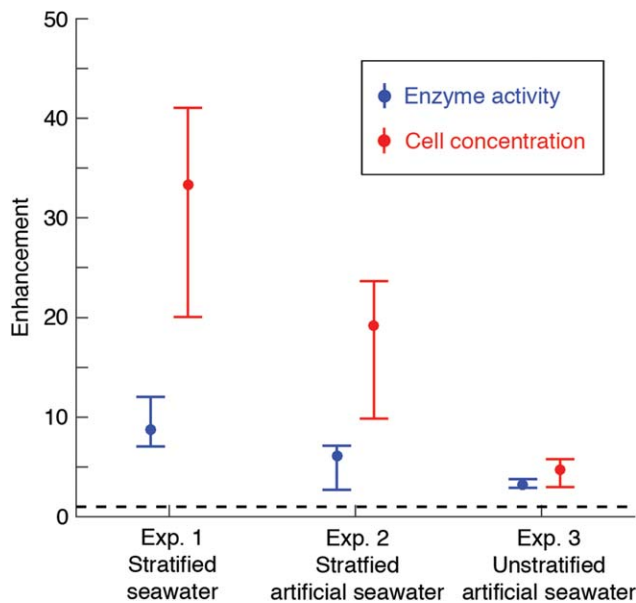


Fig. 3. Comparative enhancements of enzyme activities and cell concentrations for the two stratified experiments (Exps. 1 and 2) and the unstratified control (Exp. 3) at the density interface in the stratified tanks (and at an equivalent depth for the unstratified control) ~ 1.5 h after aggregate addition. Error bars show enhancement given 15th and 85th percentile baselines. Dashed horizontal line shows an enhancement value of 1 (i.e., no enhancement over baseline).

added to the tank. An enhancement factor of 1 thus represents no increase relative to initial values.

Results

Addition of diatom aggregates (formed with either natural or artificial seawater) led to aggregate accumulation at the density interface for 100s of seconds (Fig. 2A,D) for both of the experiments in the stratified tank (Exps. 1 and 2). This extended residence time of aggregates at a sharp density gradient has been previously investigated, and is likely related to the time required for diffusive exchange of lower-density fluid within the aggregate interior for the higher-density water of the bottom layer of the tank (Prairie et al. 2013). By contrast, in the unstratified control tank (Exp. 3), the aggregates sank through the tank volume without visible delay at any point (Fig. 2G).

In the two stratified experiments (Exps. 1 and 2), when the aggregate layer formed at the density interface, enzyme activity was enhanced by a factor of more than 20 and microbial concentration was enhanced by a factor of more than 40 at the location of the particle layer compared to the median baseline value taken before aggregates were added to the tank (Fig. 2B,C,E,F; see Supporting Information Table 2 for specific values of cell counts and enzyme activities). This enhancement, moreover, persisted over time and was measurable at the density interface ~ 1.5 h after aggregates were added to the tank, long after the aggregates had sunk to the

tank bottom (approximately 10 times longer than the duration of the thin layer itself—that is, the length of time that visible aggregates resided at the density gradient). The final median enhancement in cell concentration was 33.3 and 19.2 in Experiments 1 and 2, respectively, and the final median enhancement in enzyme activity was 8.7 and 6.1 (Fig. 3). Addition of aggregates to the unstratified control tank lacking a density gradient (Exp. 3) produced some enhancements of microbial enzyme activity and cell concentrations, but these enhancements were comparatively less than those for the stratified experiments, and there was no depth-specific pattern (Fig. 2H,I). There were also measurable enhancements in the unstratified tank 1.5 h after aggregates were added to the tank (Fig. 3), but again the enhancements were relatively modest compared to the stratified experiments, with final median enhancement in cell concentration and enzyme activity of 4.8 and 3.2, respectively. The additional control experiment with a stratified tank and no aggregates (Exp. 4) showed no enhancements of cell concentrations or enzyme activities (Supporting Information Table 2).

Discussion

Marine aggregates—including those formed from diatom cultures—typically contain high concentrations of bacterial cells that exhibit high rates of enzyme activities (e.g., Grossart et al. 2007). These experiments demonstrate that this enhancement of bacterial activity can be compounded within aggregate thin layers, where concentrations of aggregates are many times background levels. Furthermore, our results suggest that this enhanced bacterial activity can have a “memory effect,” persisting long after the aggregate layers are gone; although the thin layers were relatively ephemeral in our experiments, the enhancement of bacterial abundance and activity persisted over 10 times the duration of the aggregate thin layers at the density gradient in both stratified experiments.

The enhancement of both cell concentrations and enzyme activities long after the aggregate layer dispersed suggest that this “memory effect” is likely due to aggregate-associated microbes detaching from aggregates (Kjørboe et al. 2003; Grossart et al. 2007) during the time they were suspended at the density interface. Although we did not visually observe any changes in aggregate size at the density interface, small fragments of aggregates might also have been left at the interface, contributing to the accumulation of bacterial cells. The elevated microbial activity measured at the interface may thus result from accumulation of bacteria that possess cell-surface attached extracellular enzymes; additionally, extracellular enzymes may have been excreted from aggregate-associated cells into the water column (Ziervogel and Arnosti 2008; Ziervogel et al. 2010) and left behind at the interface once the aggregates sank to the bottom of the

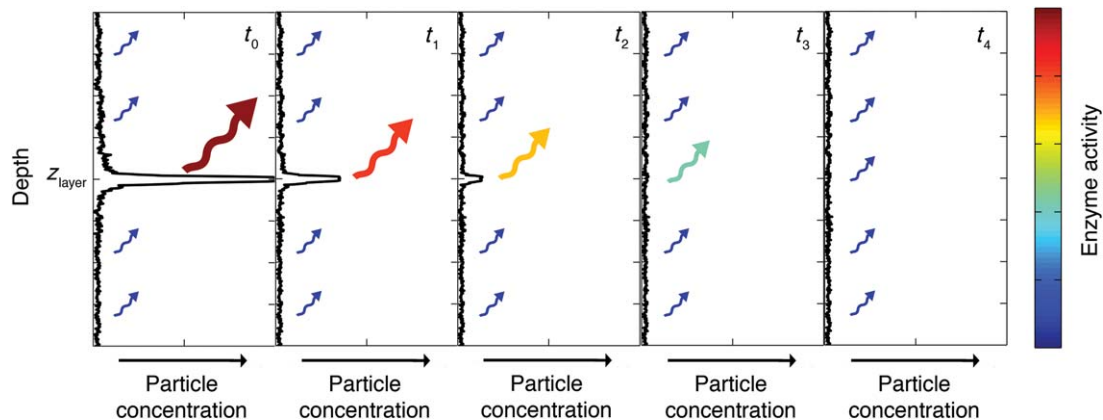


Fig. 4. Schematic demonstrating enhancement of microbial extracellular enzymatic activity (represented by both color bar and arrow size) at the depth of an aggregate thin layer (z_{layer}) at five different times (t_0 – t_4) during the transition from maximum particle concentration to dissipation of the thin layer. Black curves represent subsequent profiles of particle concentration vs. depth.

tank. Free enzymes have been reported to make a major contribution to enzymatic activity in the deep ocean (Balter et al. 2010); transient aggregate thin layers may be one source of such enzymes. In the environment, free enzymes produced by bacteria (Ziervogel and Arnosti 2008) can potentially retain activity in the water column for hours to days (Ziervogel et al. 2010).

Particle layers in the ocean can thus lead to accumulations of both bacteria and free enzymes, with the potential to significantly alter the rates of local carbon transformation for time periods much longer than the persistence of the particle patches themselves (Fig. 4). Depending on the time-scale between the enzymatic production and respiration of low molecular weight substrates, the consequences of these vertical patches for carbon cycling in the ocean could be considerable. As an example, enhanced enzymatic production of readily metabolized substrates (amino acids, simple sugars) from complex organic matter in such a thin layer could lead to localized increases in the rate of respiration of organic carbon to CO_2 , since low molecular weight substrates are readily respired in the ocean (e.g., Skoog et al. 1999).

The extent of enhancement of bacterial activity associated with aggregate layers is likely to vary substantially under different biological and environmental conditions, since bacterial community composition changes with phytoplankton growth phase, and phytoplankton species host different bacterial communities (e.g., Grossart et al. 2005). Indeed, given that the majority of bacteria in our experiments originated from the phytoplankton cultures from which the aggregates were formed, it is not surprising that we observed different magnitudes of enhancement in both bacterial cell counts and enzyme activity in the two stratified experiments. Moreover, in natural environments, processes such as small-scale turbulence and interactions with grazers may result in fragmentation of aggregates (Goldthwait et al. 2005), which will

in turn affect particle settling speeds and rates of remineralization by bacterial communities.

The persistent microbial “footprint” observed in the wake of the aggregate thin layers in our experiments has potentially important implications for a range of microbially catalyzed biogeochemical processes. “Episodic” organic matter export may be linked to specific features of nitrite maxima in the water column (Santoro et al. 2013); rates of nitrification and nitrite concentrations have also been linked along density horizons in the northeast Pacific Ocean (Smith et al. 2016). The heterogeneity of these bacterial-aggregate interactions may help provide an explanation for the spatial and temporal variability in carbon flux observed in the field (Buesseler et al. 2009; Marsay et al. 2015).

Our data also suggest a potential mechanism by which particle-associated bacteria can become redistributed in the ocean, consistent with observations from coastal California (Cram et al. 2015). Moreover, the detachment of bacteria from sinking aggregates can help shape the composition of the remaining aggregate-associated community. Analysis of sinking aggregates collected in situ at several depths in the Atlantic Ocean showed that in the upper water column, the composition of the aggregate-associated community was similar to the free-living community, whereas at greater depths, the aggregate-associated community had changed, and its composition was dominated by specific fractions of the initially attached community (Thiele et al. 2015).

Because of the extremely sharp density gradient in our experimental setup and the release of aggregates in a single pulse, the particle layers in our experiments were on the order of cms thick and persisted for only 100s of seconds. However, natural particle layers in the coastal ocean have been observed to be a meter or more thick and can persist for over a day. This extended residence time may be due to naturally formed aggregates typically having densities that are considerably less than those formed in the lab (Prairie

et al. 2013), or the presence of transparent exopolymeric particles as components of the aggregates, permitting them to reach neutral buoyancy (Alldredge et al. 2002). Under such conditions, the timescales over which aggregates remain at a density interface is considerably longer, and could lead to even greater enhancement of organisms and enzymes at a thin layer compared to the surrounding water column. This study provides experimental evidence of “footprints” of enhanced bacterial activity that may arise from aggregate thin layers; future measurements of these interactions in the field will be important to understand the implications of these results in the context of natural environmental conditions and variable microbial and planktonic communities.

References

- Allredge, A. L., and others. 2002. Occurrence and mechanisms of formation of a dramatic thin layer of marine snow in a shallow Pacific fjord. *Mar. Ecol. Prog. Ser.* **233**: 1–12. doi:10.3354/meps233001
- Arnosti, C. 2011. Microbial extracellular enzymes and the marine carbon cycle. *Annu. Rev. Mar. Sci.* **3**: 401–425. doi:10.1146/annurev-marine-120709-142731
- Azam, F., and R. A. Long. 2001. Sea snow microcosms. *Nature* **414**: 495–498. doi:10.1038/35107174
- Balter, F., J. Aristegui, J. M. Gasol, E. Sintes, H. M. van Aken, and G. J. Herndl. 2010. High dissolved extracellular enzyme activity in the deep central Atlantic Ocean. *Aquat. Microb. Ecol.* **58**: 287–302. doi:10.3354/ame01377
- Buesseler, K. O., S. Pike, K. Maiti, C. H. Lamborg, D. A. Siegel, and T. W. Trull. 2009. Thorium-234 as a tracer of spatial, temporal and vertical variability in particle flux in the North Pacific. *Deep-Sea Res. Part I* **56**: 1143–1167. doi:10.1016/j.dsr.2009.04.001
- Camassa, R., S. Khatri, R. M. McLaughlin, J. C. Prairie, B. L. White, and S. Yu. 2013. Retention and entrainment effects: Experiments and theory for porous spheres settling in sharply stratified fluids. *Phys. Fluids* **25**: 081701. doi:10.1063/1.4819407
- Camassa, R., Z. Lin, R. M. McLaughlin, K. Mertens, C. Tzou, J. Walsh, and B. White. 2016. Optimal mixing of buoyant jets and plumes in stratified fluids: Theory and experiments. *J. Fluid Mech.* **790**: 71–103. doi:10.1017/jfm.2015.720
- Cram, J. A., C.-E. T. Chow, R. Sachdeva, D. M. Needham, A. E. Parada, J. A. Steele, and J. A. Fuhrman. 2015. Seasonal and interannual variability of the marine bacterioplankton community throughout the water column over ten years. *ISME J.* **9**: 563–580. doi:10.1038/ismej.2014.153
- DeLong, E. F., D. G. Franks, and A. L. Alldredge. 1993. Phylogenetic diversity of aggregate-attached vs. free-living marine bacterial assemblages. *Limnol. Oceanogr.* **38**: 924–934. doi:10.4319/lo.1993.38.5.0924
- Ducklow, H. W., D. K. Steinberg, and K. O. Buessler. 2001. Upper ocean carbon export and the biological pump. *Oceanography* **14**: 50–58. doi:10.5670/oceanog.2001.06
- Franks, P. J. S. 1995. Thin layers of phytoplankton: A model of formation by near-inertial wave shear. *Deep-Sea Res. Part I* **42**: 75–91. doi:10.1016/0967-0637(94)00028-Q
- Goldthwait, S. A., C. A. Carlson, G. K. Henderson, and A. L. Alldredge. 2005. Effects of physical fragmentation on remineralization of marine snow. *Mar. Ecol. Prog. Ser.* **305**: 59–65. doi:10.3354/meps305059
- Grossart, H.-P., F. Levold, M. Allgaier, M. Simon, and T. Brinkhoff. 2005. Marine diatom species harbor distinct bacterial communities. *Environ. Microbiol.* **7**: 860–873. doi:10.1111/j.1462-2920.2005.00759.x
- Grossart, H.-P., K. W. Tang, T. Kiørboe, and H. Ploug. 2007. Comparison of cell-specific activity between free-living and attached bacteria using isolates and natural assemblages. *FEMS Microbiol. Lett.* **266**: 194–200. doi:10.1111/j.1574-6968.2006.00520.x
- Hoppe, H.-G. 1983. Significance of exoenzymatic activities in the ecology of brackish water: Measurements by means of methylumbelliferyl-substrates. *Mar. Ecol. Prog. Ser.* **11**: 299–308. doi:10.3354/meps011299
- Jackson, G. A. 2004. Particle trajectories in a rotating cylinder: Implications for aggregation incubations. *Deep-Sea Res. Part I* **41**: 429–437. doi:10.1016/0967-0637(94)90089-2
- Johnson, Z. I., R. Shyam, A. E. Ritchie, C. Mioni, V. P. Lance, J. W. Murray, and E. R. Zinser. 2010. The effect of iron and light-limitation on phytoplankton communities of deep chlorophyll maxima of the western Pacific Ocean. *J. Mar. Res.* **68**: 283–308. doi:10.1357/002224010793721433
- Kiørboe, T., and G. Jackson. 2001. Marine snow, organic solute plumes, and optimal chemosensory behavior of bacteria. *Limnol. Oceanogr.* **46**: 1309–1318. doi:10.4319/lo.2001.46.6.1309
- Kiørboe, T., K. W. Tang, H.-P. Grossart, and H. Ploug. 2003. Dynamics of microbial communities on marine snow aggregates: Colonization, growth, detachment, and grazing mortality of attached bacteria. *Appl. Environ. Microbiol.* **69**: 3036–3047. doi:10.1128/AEM.69.6.3036-3047.2003
- Lin, Y., K. Gazsi, V. P. Lance, A. A. Larkin, J. W. Chandler, E. R. Zinser, and Z. I. Johnson. 2013. In situ activity of a dominant *Prochlorococcus* ecotype (eHL-II) from rRNA content and cell size. *Environ. Microbiol.* **15**: 2736–2747. doi:10.1111/1462-2920.12135
- MacIntyre, S., A. L. Alldredge, and C. C. Gotschalk. 1995. Accumulation of marine snow at density discontinuities in the water column. *Limnol. Oceanogr.* **40**: 449–468. doi:10.4319/lo.1995.40.3.0449
- Marie, D., F. Partensky, D. Vaulot, and C. P. D. Brussaard. 1999. Enumeration of phytoplankton, bacteria, and viruses in marine samples. *In* J. P. Robinson [ed.], *Current protocols in cytometry*. John Wiley & Sons.
- Marsay, C. M., R. J. Sanders, S. A. Henson, K. Pabortsava, E. P. Achterberg, and R. S. Lampitt. 2015. Attenuation of

- sinking particulate organic carbon flux through the mesopelagic ocean. *Proc. Natl. Acad. Sci. USA* **112**: 1089–1094. doi:10.1073/pnas.1415311112
- McManus, M. A., and others. 2003. Characteristics, distribution and persistence of thin layers over a 48 hour period. *Mar. Ecol. Prog. Ser.* **261**: 1–19. doi:10.3354/meps261001
- Passow, U., and C. A. Carlson. 2012. The biological pump in a high CO₂ world. *Mar. Ecol. Prog. Ser.* **470**: 249–271. doi:10.3354/meps09985
- Ploug, H., and H.-P. Grossart. 2000. Bacterial growth and grazing on diatom aggregates: Respiratory carbon turnover as a function of aggregate size and sinking velocity. *Limnol. Oceanogr.* **45**: 1467–1475. doi:10.4319/lo.2000.45.7.1467
- Prairie, J. C., and others. 2013. Delayed settling of marine snow at sharp density transitions driven by fluid entrainment and diffusion-limited retention. *Mar. Ecol. Prog. Ser.* **487**: 185–200. doi:10.3354/meps10387
- Prairie, J. C., K. Ziervogel, R. Camassa, R. M. McLaughlin, B. L. White, C. Dewald, and C. Arnosti. 2015. Delayed settling of marine snow: Effects of density gradient and particle properties and implications for carbon cycling. *Mar. Chem.* **175**: 28–38. doi:10.1016/j.marchem.2015.04.006
- Prairie, J. C., and B. L. White. 2017. A model for thin layer formation by delayed particle settling at sharp density gradients. *Cont. Shelf Res.* **133**: 37–46. doi:10.1016/j.csr.2016.12.007
- Santoro, A. E., and others. 2013. Measurements of nitrate production in and around the primary nitrate maximum in the central California Current. *Biogeosciences* **10**: 7395–7410. doi:10.5194/bg-10-7395-2013
- Shanks, A. L., and E. W. Edmondson. 1989. Laboratory-made artificial marine snow: A biological model of the real thing. *Mar. Biol.* **101**: 463–470. doi:10.1007/BF00541648
- Skoog, A., B. Biddanda, and R. Benner. 1999. Bacterial utilization of dissolved glucose in the upper water column of the Gulf of Mexico. *Limnol. Oceanogr.* **44**: 1625–1633. doi:10.4319/lo.1999.44.7.1625
- Smith, D. C., M. Simon, A. L. Alldredge, and F. Azam. 1992. Intense hydrolytic enzyme activity on marine aggregates and implications for rapid particle dissolution. *Nature* **359**: 139–142. doi:10.1038/359139a0
- Smith, J. M., J. Damashek, F. P. Chavez, and C. A. Francis. 2016. Factors influencing nitrification rates and the abundance and transcriptional activity of ammonia-oxidizing microorganisms in the dark northeast Pacific Ocean. *Limnol. Oceanogr.* **61**: 596–609. doi:10.1002/lno.10235
- Stocker, R., J. R. Seymour, A. Samadani, D. E. Hunt, and M. F. Polz. 2008. Rapid chemotactic response enables marine bacteria to exploit ephemeral microscale nutrient patches. *Proc. Natl. Acad. Sci. USA* **105**: 4209–4214. doi:10.1073/pnas.0709765105
- Thiele, S., B. M. Fuchs, R. Amann, and M. H. Iversen. 2015. Colonization in the photic zone and subsequent changes during sinking determine bacterial community composition in marine snow. *Appl. Environ. Microbiol.* **81**: 1463–1471. doi:10.1128/AEM.02570-14
- Turner, J. T. 2015. Zooplankton fecal pellets, marine snow, phytodetritus and the ocean's biological pump. *Prog. Oceanogr.* **130**: 205–248. doi:10.1016/j.pocean.2014.08.005
- Ziervogel, K., and C. Arnosti. 2008. Polysaccharide hydrolysis in aggregates and free enzyme activity in aggregate-free seawater from the north-eastern Gulf of Mexico. *Environ. Microbiol.* **10**: 289–299. doi:10.1111/j.1462-2920.2007.01451.x
- Ziervogel, K., A. D. Steen, and C. Arnosti. 2010. Changes in the spectrum and rates of extracellular enzyme activities in seawater following aggregate formation. *Biogeosciences* **7**: 1007–1017. doi:10.5194/bg-7-1007-2010

Acknowledgments

We would like to thank Stephanie O'Daly and Julia Delvalle for their help with experimental work and Claudia Falcon, Shilpa Khatri, and Chung-nan Tzou for their valuable feedback. We would also like to thank the two anonymous reviewers, whose comments greatly improved this manuscript. This work is funded primarily by NSF CMG ARC-1025523. Additional funding came from NSF DMS-1009750, NSF RTG-0943851, NSF RAPID CBE, NSF OCE-1332881, NSF DBI-0959630, NSF DMS-1417879, NSF OCE-1416665, NSF OCE-1736772, and the Office of Naval Research (grant DURIP N00014-12-10749).

Submitted 23 December 2016

Revised 26 June 2017; 19 September 2017

Accepted 25 September 2017